Structural and Chemical Analyses of an Intergranular Film in Hot-Pressed Silicon Carbide

Xiao Feng Zhang[1], Qing Yang[2], and Lutgard C. De Jonghe[1,2]

[1] Materials Sciences Division,

Lawrence Berkeley National Laboratory, Berkeley, CA 94720

and

[2] Department of Materials Science and Engineering, University of California at Berkeley,

Berkeley, CA 94720

Abstract

A detailed structural and chemical characterization was performed on a ~110 nm wide intergranular film and the associated triple-junction phases in a polycrystalline SiC prepared by hot pressing with aluminum (Al), boron (B), and carbon (C) sintering additives. Selected-area electron diffraction and chemical microanalysis provided unambiguous evidence for the presence of an Al_2OC-type phase as the intergranular film and an Al-rich mullite phase in the associated triple pocket. Structure relationships between the two phases were determined. The observed distribution of the SiC content in the intergranular film and the associated triple-junction phases supported a solution-precipitation transport mechanism during hot pressing.

Keywords: SiC, Intergranular film, Triple-junction, TEM, EDS

I. Introduction

The covalent nature of SiC necessitates the use of sintering additives to achieve densification at practical temperatures and pressures. In the early 1950s, Alliegro *et al*. was among the first to sinter the SiC with suitable sintering additives (Al_2O_3 or Al).[1] Later, it was found that hot pressing with B and C additions could lead to a SiC with 96% of the theoretical density,[2] or better.[3,4] While the densification mechanism was not clear, it was already known that the boron and carbon do not form intergranular films[5,6] but instead incorporate into the SiC grains in solid solution, excluding a liquid phase densification process. High sintering temperatures, usually above 2000 ^{o}C, are required for the solid-phase sintering. Al or Al-containing additives substantially lowered the sintering temperature by as much as 300 ^{o}C,[1,3,4,7-13] due to the formation of Al-rich liquid phases that promote densification.[7,14-16] In fact, a combination of Al, B and C was found to be effective in densifying SiC at about 1900 ^{o}C, and the resulting materials possessed quite promising mechanical properties.[9,1417] For example, a high fracture toughness of 9 MPa.m$^{1/2}$ was achieved in a hot-pressed SiC.[17,18]

Because of the presence of liquid phases, about 1 nm thick, Al-containing intergranular films (IGFs) between SiC grains were formed,[7,17-22] in addition to various secondary phases, such as Al_2O_3, Al_4C_3, $Al_8B_4C_7$, Al_4O_4C, Al(Si)-O-C etc. at triple junctions.[21-23] Transmission electron microscopy (TEM) analysis revealed the amorphous nature and the Al-Si-O-C composition of these IGFs.[18-20,22] Recent studies demonstrated that the room-temperature high strength, cyclic fatigue resistance, and particularly fracture toughness of SiC hot-pressed with Al, B and C did not significantly degrade even at temperatures above 1200 ^{o}C.[24-28] Moreover, the SiC also exhibited excellent creep resistance at temperatures as high as 1500 ^{o}C.[29,30] The remarkable properties achieved when 3-5 wt% Al was incorporated could be correlated with the structural evolution of the IGFs on heat treatment.[22] Clearly, detailed information on the structure and composition of the IGFs is important in understanding and controlling mechanical properties of the material. However, quantitative characterization of the IGFs has been difficult due to their nanometer thickness: too thin to be analyzed by selected-area electron diffraction (SAED) and X-ray energy-dispersive spectroscopy (EDS)

without interference from the adjacent matrix. As a result, the presence of Si and C in IGFs could not be determined with certianty.

In this paper, a detailed structural and compositional TEM analyses is reported on a 110 nm wide IGF formed in the as-hot-pressed SiC. Unambiguous SAED and EDS analyses for this unusually wide IGF allowed unambiguous identification and analysis of the Al_2OC-SiC-based intergranular phase, and of a mullite phase for the associated triple-junction material, respectively.

II. Experimental

Submicron β-SiC (B20, H. C. Starck, Germany) starting powders were mixed with 3 wt% aluminum metal (H-3 and H-10, Valimet, Stockton, CA), 0.6 wt% boron (Callery Chemical Co, Callery, PA), and 2 wt% carbon. Apiezon wax (AVO Biddle Instruments, Blue Bell, PA) was dissolved in toluene to serve as the C source. Al, B, and β-SiC were added to the solution, and ultrasonically agitated to minimize agglomerate formation. The slurry was stir-dried, and the powder was sieved through a 200 mesh screen. Green compacts were uniaxially pressed at 35 MPa. Hot-pressing was performed at 1900°C, 50 MPa, for 1 hour in argon at 1 atmosphere. The products were highly dense (3.18 g/cm^3), and referred to as ABC-SiC.[17] 4H- and 6H-SiC phases were dominant.

Structural and chemical characterizations were carried out in a field-emission gun Philips CM200 transmission electron microscope operating at 200 kV. For compositional alalysis, an EDS system equipped with a windowless detector and ES Vision 3.0 software, issued by EMiSPEC System, Inc., was used. Boron can be detected with this EDS system. Chemical quantification, absorption and fluorescence corrections, background subtraction, and Gaussian peak-fitting were performed for the K_α peak of the elements, followed by integration of the net counts. SiC and $Al_8B_4C_7$ phases in the samples served as internal standards, and Al_2O_3 as an external standard in determining Cliff-Lorimer factors (k-factors) for quantitative analysis of Al-, O-, Si-, and C-containing phases. The absolute uncertainty in the k-factors (relative to Si) was between 10 and 15 %.

III. Results and Discussion

While ~0.8-3 nm wide amorphous IGFs are prevalent in ABC-SiC samples,[22] Fig. 1 shows an exception: a ~110 nm wide IGF encountered in an as-hot-pressed ABC-SiC sample. Two associated triple-junction particles are seen with low dihedral angles, implying good wettability by the liquid of the SiC grain surfaces during the liquid phase sintering.[23] The fortuitously wide IGF found here offered a unique opportunity for characterizing the structure and composition using traditional selected-area electron diffraction (SAED) and EDS, without concern about interference from the adjacent matrix grains.

Fig. 1: Bright-field image showing an unusually wide, ~110 nm intergranular film in as-hot-pressed ABC-SiC. Two associated triple pockets were marked as Pocket I and Pocket II. EDS microanalyses were performed along the intergranular film and in triple-junctions. Some analyzed spots and corresponding compositions has been marked. The experimentally determined Al and Si site densities in the grain boundary film (N_{Al}^{GB}, N_{Si}^{GB}) are listed at the lower-left corner of the figure.

Some spots are marked in the IGF and the associated triple-junction material, Fig. 1, where EDS microanalyses were performed using a 17 nm diameter probe, small enough to probe the IGF without including any the flanking SiC grains. A typical EDS spectrum obtained from the IGF is shown in Fig. 2a. It is quite obvious that the IGF was composed of Si-Al-C-O; no boron was detected. It should be noted that the carbon peak in the spectrum was higher than it should be due to the hydrocarbon surface contamination during the EDS spectrum acquisition. The presence of C contamination was evident in the EDS spectrum acquired from the adjacent SiC grain as shown in Fig. 2b, where the C to Si atom ratio is 2.3, instead of 1.0 for SiC. The SiC grain bulk could therefore be used as an internal standard to make a correction for carbon content. Note that the EDS spectrum in Fig. 2b was acquired at a spot about 50 nm away from the IGF/SiC interface, close enough to provide identical acquisition conditions for spectra in Fig. 2a and Fig. 2b. Fig. 2c shows an EDS spectrum acquired at the interface between

the IGF and adjacent SiC, *i.e.*, the beam illuminated both the IGF and SiC matrix. The peak positions and intensities in Fig. 2c resemble very well those in typical EDS spectra obtained from regions containing ~1 nm IGF segments.[22,23] This agreement indicated that the 110 nm wide IGF studied in the present paper has a composition similar to that of ~1 nm wide IGFs.

Fig. 2: EDS spectra acquired from (a), within grain boundary film; (b), inside the SiC matrix; and (c), interface between the grain boundary film and the SiC matrix. The chemical compositions were determined after correction for the hydrocarbon contamination.

The compositions determined at two locations in the IGF were normalized to $Al_{2.0}$ and marked in Fig. 1. Al and Si site densities in the IGF (N_{Al}^{IGF} and N_{Si}^{IGF}) were determined using the ratio between Al- and Si-peak intensities:

$$N_{Al}^{IGF} = k_{AlSi}\frac{A_{Si}}{A_{Al}}\frac{I_{Al}^{IGF}}{I_{Si}^{G}}\times N_{Si}^{G}$$

$$N_{Si}^{IGF} = \frac{I_{Si}^{IGF}}{I_{Si}^{G}}\times N_{Si}^{G}$$

where k_{AlSi} denotes the k-factor, A_{Si} and A_{Al} the atomic weight, I_{Al}^{IGF} and I_{Si}^{IGF} the Al and Si peak intensities from the IGF, I_{Si}^{G} the Si peak intensity from the SiC, and N_{Si}^{G} the site density of Si in SiC (16.1 nm^{-3} for 4H-, or 6H-SiC). On average, we obtained N_{Al}^{IGF} = 9.6 nm^{-3}, and N_{Si}^{IGF} = 11.8 nm^{-3}, as marked in Fig. 1. The value of N_{Al}^{IGF} was in a good agreement with that derived for nanometer-wide IGFs.[22] Based on the EDS analyses, the average composition for the IGF was found to be close to $Al_2OC{\cdot}2.5SiC$, a solid solution between Al_2OC and SiC. This kind of solid solution phase has been proposed and studied in earlier work.[31,32] The IGF composition determined here provides unambiguous evidence for the presence of Si in the Al_2OC grain boundary phase, as was suggested in a previous paper about high-resolution electron microscopy study and indirect EDS analyses of the nanometer thick IGFs.[22]

Fig. 3a and Fig. 3b show EDS spectra obtained in the center, and at the corner of the triple–particle in Pocket I marked in Fig. 1. The corresponding compositions have been marked in Fig. 1. The increase in the O/Al atom ratio was significant in the triple junction particle, actually about 4-times higher than that in the IGF. This substantial difference between O/Al ratios could not be accounted for by a change in k-factor with foil thickness.[33] The composition in the center region of the particle was determined to be $Al_{2.0}Si_{1.0}O_{3.7}C_{0.7}$, which could also be written as $5.7Al_2O_3{\cdot}2SiO_2{\cdot}3.7SiC$. This composition actually implied an Al-rich mullite phase, mixed with SiC, as will be discussed later. It is interesting to note that the Si content decreased sharply at the corner of the particle, where the composition was closer to Al_2O_3, Fig. 3b. According to Kriven *et al*., high Al_2O_3 content in mullite resulted in precipitation of α-Al_2O_3 as a primary phase.[34] This conclusion is consistent to our observation.

Fig. 3: EDS spectra acquired from (a), center of Pocket I; (b), corner of Pocket I; and (c), center of Pocket II. The determined chemical compositions are marked in Fig. 1.

Clearly, the triple-phase in Pocket I was different from that in the IGF. In contrast, the particle in Pocket II (Fig. 1) possessed a similar composition to that of the IGF, Fig. 3c. The composition was determined to be $Al_{2.0}O_{0.9}C_{1.1}Si_{0.05}$, essentially the same type of Al_2OC-SiC phase as in the IGF, except that the SiC in solution in the Pocket II particle was much less. The common SiC components found in the IGF and in the triple-junction phases confirmed the solution-precipitation mechanism suggested for SiC sintering.[7,14-17] Moreover, the EDS analyses reported here strengthened the conclusion made in a previous paper that the compositions of IGF and the associated triple-junction phases is not necessarily the same.[23]

The phases determined by EDS were analyzed by SAED, as shown in Fig. 4. Fig. 4a shows an SAED pattern taken from the IGF. The 110 nm wide IGF had crystallized, in contrast to the amorphous structure of the prevalent nanometer-wide IGFs in the very same sample. The d-spacing of some reflections in Fig. 4a are marked, which matches well with X-ray powder diffraction data for α'-Al_2OC phase.[35] The α'-Al_2OC phase was

regarded as a variant of the α-Al_2OC, corresponding to a long-range ordering based on the 2H wurtzite structure.[35] The Al_2OC phase was known to be stabilized by SiC in solid solution,[31,32] therefore the Al_2OC-SiC composition determined for the IGF (Fig. 2a) was as expected.

Fig. 4: (a), SAED pattern taken in the intergranular film. Values of d-spacing for some reflections are marked, which match the α'-Al_2OC structure. (b), SAED pattern taken in the central region of Pocket I. The pattern corresponds to a mullite [010]* projection with incommensurate satellites among the main reflections. The projection unit cells outlined in (a) and (b) reveal an orientation relationship between the grain boundary film and the secondary phase in Pocket I.

Fig. 4b shows an SAED pattern obtained from the center region of the triple-junction particle in Pocket I (Fig. 1). The pattern shows the [010]* zone-axis projection of a $3Al_2O_3 \cdot 2SiO_2$ (3:2) mullite-derived structure. The projected unit cell is outlined, and (200) and (001) main reflections are marked. Incommensurate satellites were recognized among main reflections, resembling 'd' or 'e' modulations reported by Cameron.[36] Instead of a 3:2 ratio between Al_2O_3 and SiO_2 for the standard 3:2 mullite, the molar ratio in the triple-particle studied here was about 2.9. According to Cameron, an incommensurate superlattice appeared when the molar ratio between Al_2O_3 and SiO_2 falls between 2.15 – 3.17,[36] due to the ordered oxygen vacancies.[36,37]

Since the two SAED patterns in Fig. 4 were taken at the same TEM sample orientation, the projected unit cells outlined in Fig. 4a and Fig. 4b demonstrated a fixed orientation relationship and a good lattice match between the IGF and the triple-junction phase in Pocket I.

The formation of the Al_2OC-SiC phase in the wide IGF was apparently a result of considerable SiC dissolution in the Al-O-C liquid during liquid phase sintering. Initially, the Al and C from sintering additives and SiO_2 from oxidation layers on SiC grain surface are likely to form a AlOSiC liquid phase. The Al_2OC phase can coexisted with liquid at 1900 ^oC according to phase diagram,[38] and available experimental reports,[10,39] but a solid solution between Al_2OC and SiC was preferred in Si-Al-C-O system, since

SiC component can stabilize Al_2OC.[10,31,32] At the same time, the composition in Pocket I (Fig. 1) favored formation of the mullite-derived phase. A clear boundary was discerned by SAED between the Pocket I phase and the IGF phase. For most of the nanometer-wide IGFs in the same sample, Al-O-Si-C constituents were detected,[22] similar to the composition for the ~110 nm IGF. However, the nanometer-wide dimension constrained these IGFs initially to an amorphous structure after cooling from the processing temperature. Post-annealing at temperatures below 1700 ^oC does lead to crystallization of these amorphous nanometer-wide grain boundary films, resulting in formation of Al_2OC-SiC aluminosilicates[22] with the same structure that is observed for the ~110 nm wide IGF studied here.

It should be pointed out that the IGF studied here is unusual because of its ~110 nm width and crystalline structure, in contrast to the ~1 nm wide, amorphous IGFs ubiquitous in as-hot-pressed ABC-SiC. Although only a very limited number of such unusually wide IGFs have been found so far, the chemical analysis agreed well with previous conclusions based on point-EDS microanalysis on nanometer-wide IGFs. The agreement was also supported by the EDS spectrum shown in Fig. 2c. It is believed that the Al_2OC-SiC phase determined for the wide IGF represents at least a significant fraction of the crystalline IGF phases formed in annealed ABC-SiC.

The significance of the current work is to provide unambiguous answers to several longstanding questions about IGF structure and composition, SiC dissolution in IGFs, and relationships between IGF and associated triple-junction phases.

IV. Conclusion

A ~110 nm wide intergranular film was found in a hot-pressed ABC-SiC sample. The unusually wide IGF allowed for direct structural and chemical characterization using selected-area electron diffraction and EDS chemical analysis. The results demonstrate unambiguously that the IGF possessed a crystalline, α'-Al_2OC-based structure with a considerable amount of SiC in solid solution. The triple-junction particle at one end of the IGF was concluded to be similar to that of the IGF, whereas the triple-junction phase at another end was determined to have a mullite-derived structure and composition. The

configuration confirmed that the structure and composition of IGFs in ABC-SiC may not necessarily be identical to that of the associated triple-junction particles. The presence of a significant SiC content in the IGF and in associated triple-junction phases support the solution-precipitation liquid-phase sintering mechanism during hot pressing of ABC-SiC. The structure and composition determined for the unusually wide IGF showed essential agreement with that of the nanometer-wide crystalline IGFs which were prevalent in ABC-SiC after post-annealing.

Acknowledgment:

This work was supported by the Director, Office of Science, Office of Basic Energy Sciences, Materials Sciences Division of the U.S. Department of Energy under Contract No. DE-AC03-76SF0098. Part of this work was made possible through the use of the National Center for Electron Microscopy facility at the Lawrence Berkeley National Laboratory.

References

[1]R.A. Alliegro, L.B. Coffin, and J.R. Tinklepaugh, "Pressure-Sintered Silicon Carbide," *J. Am. Ceram. Soc*., **39** [11] 386-89 (1956).

[2]S. Prochazka, and R.M. Scanlan, "Effect of Boron and Carbon on Sintering of SiC," *J. Am. Ceram. Soc*., **58** [1-2] 72 (1975).

[3]R.M. Williams, B.N. Juterbock, S.S. Shinozaki, C.R. Peters, and T.J. Whalen, "Effects of Sintering Temperatures on the Physical and Crystallographic Properties of β-SiC," *Am. Ceram. Soc. Bull.*, **64** [10] 1385-89 (1985).

[4]T. Nagano, K. Kaneko, G.-D. Zhan, and M. Mitomo, "Effect of Atmosphere on Weight Loss in Sintered Silicon Carbide During Heat Treatment," *J. Am. Ceram. Soc*., **83** [11] 2781-87 (2000).

[5]R. Hamminger, G. Grathwohl, and F. Thummler, "Microanalytical Investigation of Sintered SiC, II," *J. Mater. Sci.*, **18** 3154-60 (1983).

[6]J. E. Lane, C.H. Carter, and R. F. Davis, "Kinetics and Mechanisms of High Temperature Creep in Silicon Carbide: III, Sintered α-Silicon Carbide," *J. Am. Ceram. Soc*., **71** [4] 281-95 (1988).

[7]F.F. Lange, "Hot-Pressing Behavior of Silicon Carbide Powders with Additions of Aluminum Oxide," *J. Mater. Sci.*, **10** 314-20 (1975).

[8]M. Omori, and H. Takei, "Pressureless Sintering of Silicon Carbide," *J. Am. Ceram. Soc*., **65** [6] C-923 (1982).

[9]H. Tanaka, Y. Inomata, K. Hara, and H. Hasegawa, "Normal Sintering of Al-doped β-SiC," *J. Mater. Sci. Lett.,* **4** 315-17 (1985).

[10]J.-L. Huang, A.C. Hurford, R.A. Cutler, and A.V. Virkar, "Sintering Behavior and Properties of SiCAlON Ceramics," *J. Mater. Sci. Lett.,* **21** 1448-56 (1986).

[11]M.A. Mulla, and V.D. Krstic, "Low Temperature Pressureless Sintering of β-Silicon Carbide with Aluminum Oxide and Yttrium Oxide Additions," *Am. Ceram. Bull.*, **70** 439-43 (1991).

[12]N. P. Padture, "*In Situ*-Toughened Silicon Carbide," *J. Am. Ceram. Soc.*, **77** [2] 519-23 (1994).

[13]H. Tanaka, and Y. Zhou, "Low Temperature Sintering and Elongated Grain Growth of 6H-SiC Powder with AlB_2 and C additives," *J. Mater. Res.* **4** [2] 518-22 (1999).

[14]B.W. Lin, M. Imai, T. Yano, and T. Iseki, "Hot-Pressing of β-SiC Powder with Al-B-C Additives," *J. Am. Ceram. Soc.*, **69** [4] C-67-C-68 (1986).

[15]A.K. Misra, "Thermochemical Analysis of the Silicon Carbide-Alumina Reaction with Reference to Liquid-Phase Sintering of Silicon Carbide," *J. Am. Ceram. Soc.*, **74** [2] 345-51 (1991).

[16]Y. Zhou, H. Tanaka, S. Otani, and Y. Bando, "Low Temperature Pressureless Sintering of α-SiC with Al_4C_3-B_4C-C Additions," *J. Am. Ceram. Soc.*, **82** [8] 1959-64 (1999).

[17]J.J. Cao, W.J. MoberlyChan, L.C. De Jonghe, C.J. Gilbert, and R.O. Ritchie, "In Situ Toughened Silicon Carbide with Al-B-C Additions," *J. Am. Ceram. Soc.*, **79** [2] 461-69 (1996).

[18]W.J. MoberlyChan, J.J. Cao, and L.C. De Jonghe, "The role of the Amorphous Grain Boundaries and the β-α Transformation in Toughening SiC," *Acta Mater.*, **46** [5] 1625-35 (1998).

[19]R. Hamminger, G. Grathwohl, and F. Thummler, "Microanalytical Investigation of Sintered SiC, I," *J. Mater. Sci.*, **18** 353-64 (1983).

[20]L. Sigl, and H.-J. Kleebe, "Core/Rim Structure of Liquid-Phase-Sintered Silicon Carbide," *J. Am. Ceram. Soc.*, **76** [3] 773-76 (1993).

[21]W.J. MoberlyChan, and L.C. De Jonghe, "Controlling Interface Chemistry and Structure to Process and Toughen Silicon Carbide," *Acta Mater.*, **46** [7] 2471-77 (1998).

[22]X.F. Zhang, M.E. Sixta, and L.C. De Jonghe, "Grain Boundary Evolution in Hot-Pressed ABC-SiC," *J. Am. Ceram. Soc.*, **83** [11] 2813-20 (2000).

[23]X.F. Zhang, M.E. Sixta, and L.C. De Jonghe, "Secondary Phases in Hot-Pressed ABC-Silicon Carbide," *J. Am. Ceram*. Soc., **84** [4] 813-20 (2001).

[24]D. Chen, C.J. Gilbert, X.F. Zhang, and R.O. Ritchie, "High-temperature cyclic fatigue-crack growth behavior in an in situ toughened silicon carbide," *Acta Materialia* **48** [3] 659-74 (2000).

[25]D. Chen, X.F. Zhang, and R.O. Ritchie, "Effects of grain-boundary structure on the strength, toughness and cyclic fatigue properties of monolithic silicon carbide," *J. Am. Ceram. Soc.*,**83** [8] 2079-81 (2000).

[26]D. Chen, M.E. Sixta, X.F. Zhang, L.C. De Jonghe, and R.O. Ritchie, "Role of the Grain-Boundary Phase on the Elevated-Temperature Strength, Toughness, Fatigue and Creep Resistance of Silicon Carbide Sintered with Al, B and C", *Acta Materialia*, in review.

[27]X.F. Zhang, M.E. Sixta, and L.C. De Jonghe, "Nano-Precipitation in Hot-pressed Silicon Carbide," *J. Mater. Sci.*, in press.

[28]R.O. Ritchie, D. Chen, and X.F. Zhang, "Fatigue of Ceramics at Elevated Temperatures: Microstructural Design for Optimal Performance", *International Journal of Materials and Product Technology*, in press.

[29]X.F. Zhang, M.E. Sixta, and L.C. De Jonghe, "Diffusion-Controlled Responses to Heat Treatment of Toughened Silicon Carbide", *Defect and Diffusion Forum*, **186-187** 45-60 (2000).

[30]M.E. Sixta, X.F. Zhang, and L.C. De Jonghe, "Creep of an *In-Situ* Toughened SiC", *J. Am. Ceram. Soc.*, in press.

[31]I.B. Cutler, P.D. Miller, W. Rafaniello, H.K. Park, D.P. Thompson, and K.H. Jack, "New Materials in the Si-C-Al-O-N and Related Systems," *Nature*, **275** 434-35 (1978).

[32]F. Babonneau, G. D. Soraru, K. J. Thorne, and J.D. Mackenzie, "Chemical Characterization of Si-Al-C-O Precursor and Its Pyrolysis," *J. Am. Ceram. Soc.*, **74** [7] 1725-28 (1991).

[33]A.D. Westwood, J.R. Michael, and M.R. Notis, "Experimental Determination of Light-Element k-Factors Using the Extrapolation Technique: Oxygen Segregation in Aluminum Nitrid," *J. Micro.*, **167**, 287-302 (1992).

[34]W.M. Kriven, and J.A. Pask, "Solid Solution Range and Microstructures of Melt-Grown Mullite," *J. Am. Ceram. Soc.*, **66** [9] 649-54 (1983).

[35]H. Yokokawa, M. Dokiya, M. Fujishige, T. Kamayama, S. Ujiie, and K. Fukuda, "X-Ray Powder Diffraction Data for Two Hexagonal Aluminum Monoxycarbide Phases," *Commu. Am. Ceram. Soc.*, C-40-4 (1982).

[36]W.E. Cameron, "Mullite: a Substituted Alumina," *Am. Mineral.*, **62**, 747-55 (1977).

[37]Y. Nakajima, and P.H. Ribbe, "Twinning and Superstructure of Al-Rich Mullite," *Am. Mineral.*, **66**, 142-7 (1981).

[38]L.M. Foster, G. Long, and M.S. Hunter, "Reactions between Aluminum Oxide and Carbon: The Al_2O_3-Al_4C_3 Phase Diagram," *J. Am. Ceram. Soc.*, **39** [1] 1-11 (1956).

[39]J.M. Lihrmann, T.Zambetakis, and M. Daire, "High-Temperature Behavior of the Aluminum Oxycarbide Al_2OC in the System Al_2O_3-Al_4C_3 and with Additions of Aluminum Nitride," *J. Am. Ceram. Soc.*, **72** [9] 1704-709 (1989).

Figure Captions

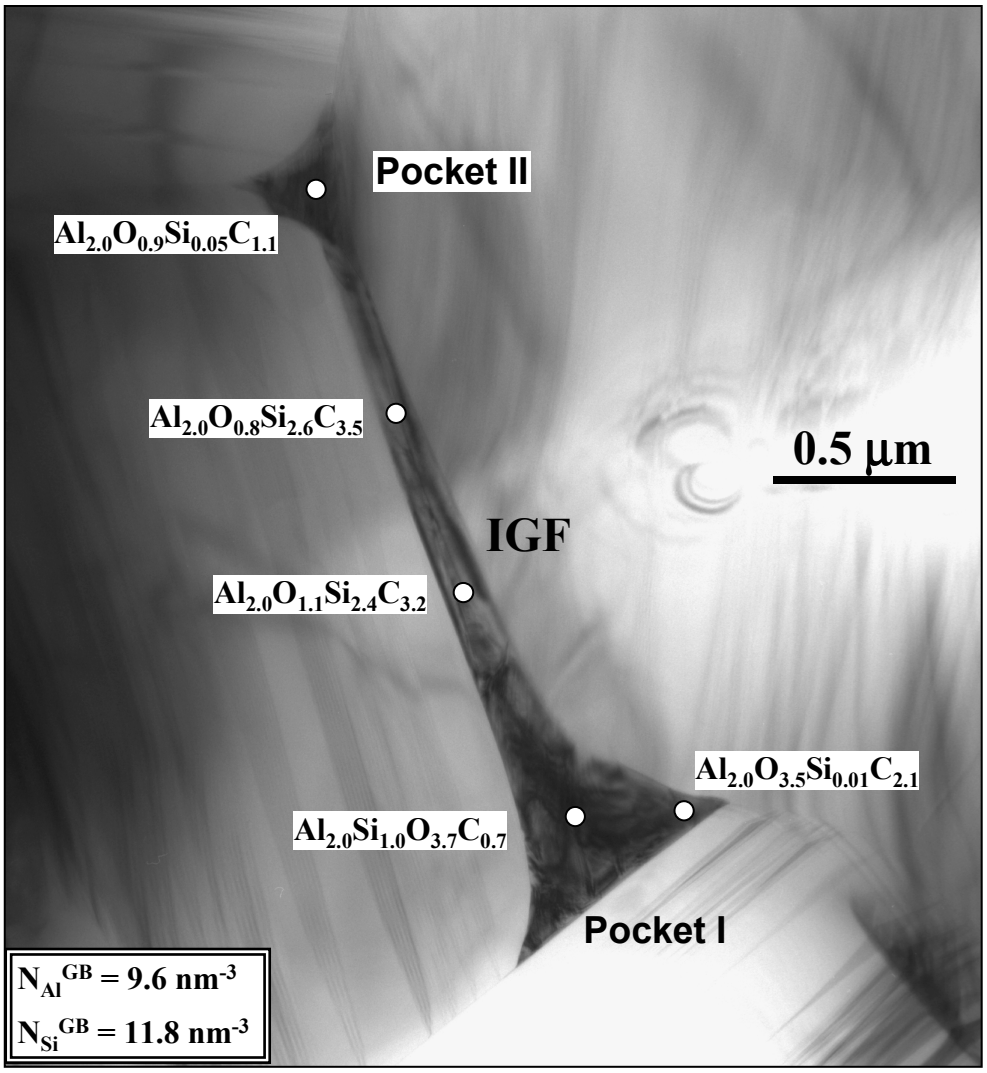

Fig. 1: Bright-field image showing an unusually wide, ~110 nm intergranular film in as-hot-pressed ABC-SiC. Two associated triple pockets were marked as Pocket I and Pocket II. EDS microanalyses were performed along the intergranular film and in triple-junctions. Some analyzed spots and corresponding compositions were marked. The experimentally determined Al and Si site densities in the grain boundary film (N_{Al}^{GB}, N_{Si}^{GB}) are listed at the lower-left corner of the figure.

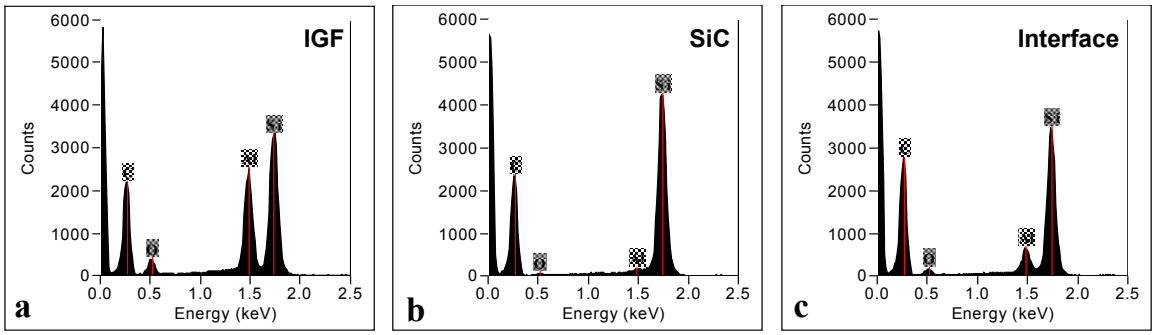

Fig. 2: EDS spectra acquired from (a), within grain boundary film; (b), inside the SiC matrix; and (c), interface between the grain boundary film and the SiC matrix. The chemical compositions were determined after correction for the hydrocarbon contamination.

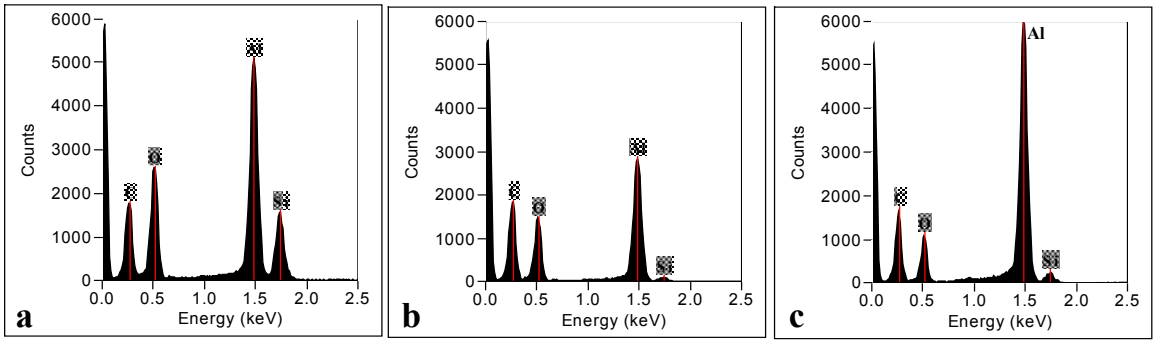

Fig. 3: EDS spectra acquired from (a), center of Pocket I; (b), corner of Pocket I; and (c), center of Pocket II. The determined chemical compositions are marked in Fig. 1.

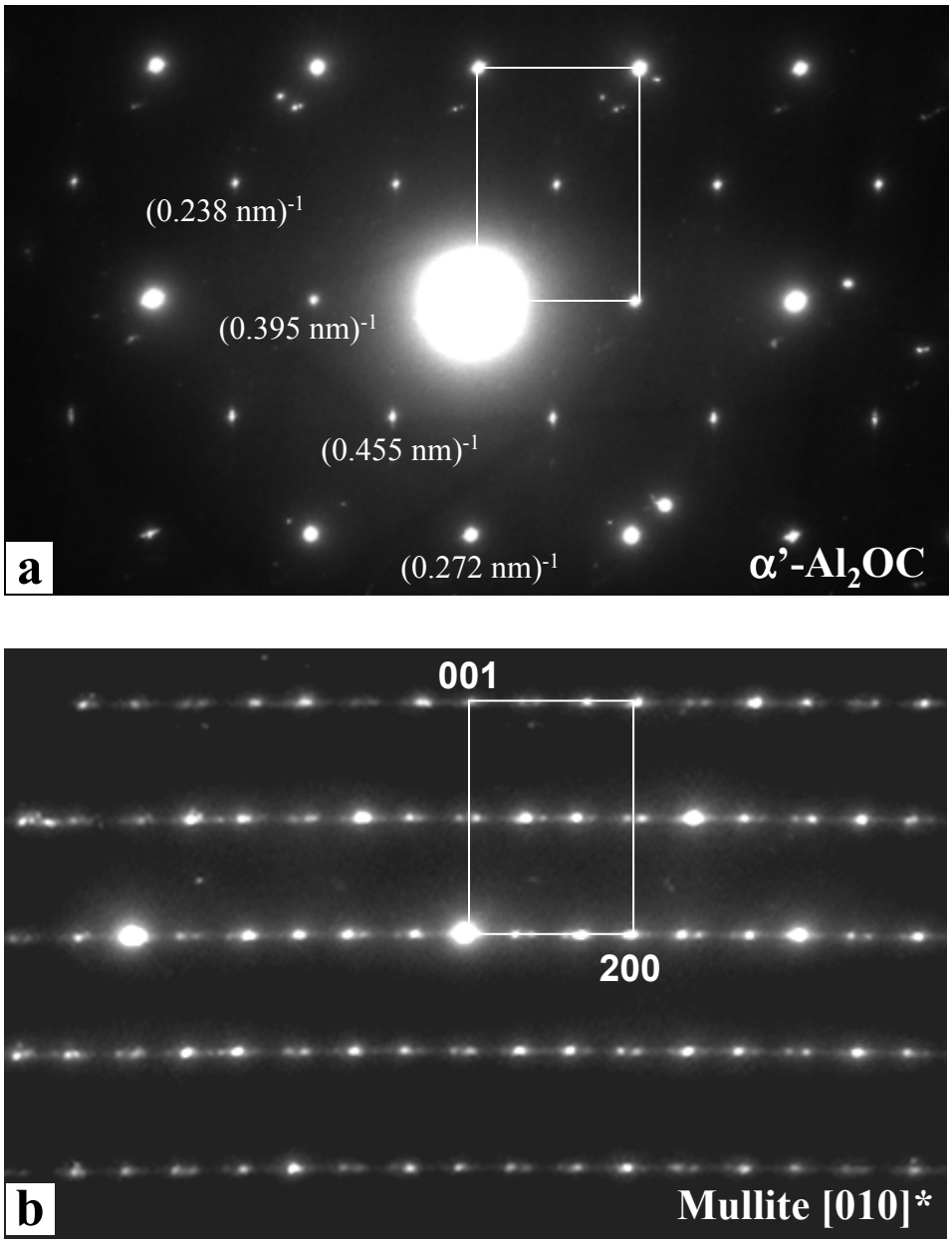

Fig. 4: (a), SAED pattern taken in the intergranular film. Values of d-spacing for some reflections are marked, which match the α'-Al_2OC structure. (b), SAED pattern taken in the central region of Pocket I. The pattern corresponds to a mullite [010]* projection with incommensurate satellites among the main reflections. The projection unit cells outlined in (a) and (b) reveal an orientation relationship between the grain boundary film and the secondary phase in Pocket I.